



**HAL**  
open science

## **Influence of a localized defect on acoustic field correlation in a reverberant medium**

Najib Abou Leyla, Emmanuel Moulin, Jamal Assaad

► **To cite this version:**

Najib Abou Leyla, Emmanuel Moulin, Jamal Assaad. Influence of a localized defect on acoustic field correlation in a reverberant medium. *Journal of Applied Physics*, 2011, 110, pp.084906-1-8. 10.1063/1.3652907. hal-00639940

**HAL Id: hal-00639940**

**<https://hal.science/hal-00639940v1>**

Submitted on 25 May 2022

**HAL** is a multi-disciplinary open access archive for the deposit and dissemination of scientific research documents, whether they are published or not. The documents may come from teaching and research institutions in France or abroad, or from public or private research centers.

L'archive ouverte pluridisciplinaire **HAL**, est destinée au dépôt et à la diffusion de documents scientifiques de niveau recherche, publiés ou non, émanant des établissements d'enseignement et de recherche français ou étrangers, des laboratoires publics ou privés.

# Influence of a localized defect on acoustic field correlation in a reverberant medium

Cite as: J. Appl. Phys. **110**, 084906 (2011); <https://doi.org/10.1063/1.3652907>

Submitted: 16 March 2011 • Accepted: 10 September 2011 • Published Online: 19 October 2011

Najib Abou Leyla, Emmanuel Moulin and Jamal Assaad



View Online



Export Citation

## ARTICLES YOU MAY BE INTERESTED IN

[Detection and localization of a defect in a reverberant plate using acoustic field correlation](#)

Journal of Applied Physics **115**, 104901 (2014); <https://doi.org/10.1063/1.4867522>

[Applicability of acoustic noise correlation for structural health monitoring in nondiffuse field conditions](#)

Applied Physics Letters **95**, 094104 (2009); <https://doi.org/10.1063/1.3200240>

[On the emergence of the Green's function in the correlations of a diffuse field](#)

The Journal of the Acoustical Society of America **110**, 3011 (2001); <https://doi.org/10.1121/1.1417528>

Lock-in Amplifiers  
up to 600 MHz



Zurich  
Instruments



## Influence of a localized defect on acoustic field correlation in a reverberant medium

Najib Abou Leyla, Emmanuel Moulin,<sup>a)</sup> and Jamal Assaad

*IEMN UMR CNRS 8520 Université de Valenciennes et du Hainaut-Cambrésis F-59313 Valenciennes cedex 9 France*

(Received 16 March 2011; accepted 10 September 2011; published online 19 October 2011)

The work presented in this paper is concerned with the fundamental study of a damage detection principle in a reverberant medium, based on ambient acoustic noise correlation. The aim here is to theoretically investigate the sensitivity of the correlation of received signals to a local defect. The acoustic reverberation in the medium is modeled by a random process and an empirical description of the defect behavior is deduced from its experimental characterization. A global parameter  $r$ , corresponding to the energy ratio between the change in the correlation function caused by the defect and the defect-free correlation, is defined and theoretically derived. It is shown to essentially depend on the reverberation properties of the medium and the relative positions of the noise source, the sensor(s) and the defect. The theoretical expression of  $r$  is experimentally validated in a particular 2D-case (metallic plate) and then used to define the detection range and the optimal placements of the sensors. © 2011 American Institute of Physics. [doi:10.1063/1.3652907]

### I. INTRODUCTION

Recent trends in theoretical research on acoustic imaging<sup>1–5</sup> are concerned with the means of performing imaging in complex media, where the time-of-flights of waves are not distinguishable and thus conventional imaging algorithms are not applicable. The bonus idea in this case is to increase the sensitivity and the spatial range of the technique by exploiting the whole “diffuse” signals rather than a few temporally localized echoes. Indeed, even a moderate local modification of the medium properties will result in significant changes in a multipaths wave propagation. The exploitation of such ideas has given birth to a range of techniques known as coda-wave interferometry or diffusing wave spectroscopy, first developed in optics and later transposed to acoustic waves.<sup>6</sup> In practice, signal cross-correlation is used to compare the waves in the reference-state medium and the waves, generated in the same conditions, in the modified medium.<sup>7,8</sup> These techniques have been successfully applied to geophysical applications<sup>9,10</sup> and to ultrasound in reverberant media.<sup>11,12</sup>

Besides, many recent studies in various application domains such as underwater acoustics<sup>13–16</sup> and seismology<sup>17–19</sup> have shown the potential of extracting information about a given medium through exploitation of the natural ambient acoustic noise present in this medium. Theoretically, in the presence of a perfectly diffuse field (spatial and temporal uniformity), it is possible to retrieve the Green’s function between two points by cross-correlating the signals received simultaneously at these points.<sup>20–23</sup> Structural health monitoring (SHM) is a more recently investigated application of this principle.<sup>24–27</sup> In particular, aeronautical structures may be good candidates for such application, since they are subject to intense acoustic noise sources during service (engines, air friction, or local aero-

acoustic effects). The work presented in this paper primarily belongs —but might not be limited— to this context.

One of the difficult points in ambient noise correlation techniques is the extreme sensitivity to the actual acoustic field conditions. In the hypothetical case of a perfectly diffuse field, the obtained correlation functions only depend on the structural properties (including possible damage) of the medium. But in other cases, the correlations are also influenced by the characteristics of the acoustic sources (position, power spectral density), which might fluctuate from one measurement to the other. In other works, this specific problem is usually bypassed either by controlling the acoustic sources or by artificially increasing the diffuse nature of the field (spatial averaging, use of chaotic-shaped media, etc.).<sup>24–26</sup> Only a few recent studies<sup>27,28</sup> have focused on directly coping with the nondiffuse nature of the field. In particular, we have proposed<sup>27,29,30</sup> the use of a “reference” sensor in order to be able to identify the acoustic source characteristics at the instant of measurement. This solution is inspired by the impact localization technique based on one-channel time reversal.<sup>31–33</sup> The reverberant nature of the propagation (considerable number of multipaths) makes indeed the dependence of the measured signals on the source characteristics potentially unequivocal. The principle is then to compare the measured correlation function to a set of baseline correlation functions stored in a database and corresponding to the most frequent source configurations.

Theoretically speaking however, the multipath propagation should be affected also by a localized change (damage) in the medium. Then the crucial point for this application is where to place the reference sensor so that it would be as insensitive as possible to a damage appearing in the part of the medium that we want to monitor (inspection area). A very simple, first-approach empirical description based on the general waveform aspects had been proposed in a previous work.<sup>27</sup> It has allowed a demonstration of the feasibility

<sup>a)</sup>Electronic mail: emmanuel.moulin@univ-valenciennes.fr

of the principle, but provided only a coarse description with actually no firm physical justification.

A more complete and rigorous physical description is given in this paper. The reverberation caused by the medium boundaries is treated as a random process, which is convenient for extracting a general behavior (in the form of expected values) of the physical phenomena involved. In this way, the envelope of the received signal can be physically related to the medium properties, and then the influence of the relative source, receiver and damage positions on the correlation function can be explicated and precisely quantified. This is the object of the first part of this paper. In the second part, the results of these theoretical developments are compared to measurements. Practical exploitation of the obtained results for the SHM system design is also proposed.

## II. THEORY

### A. Problem settings and assumptions

Let us consider a finite-size medium with characteristic dimensions much smaller than the acoustic absorption length. In the experimental study presented in Sec. III, for instance, the considered medium is an aluminum plate that might represent a part of an aeronautical shell structure. This medium is supposed to be excited by some ambient sources. We will consider in this study the simplified case of a single acoustic source ( $S$ ) and a single receiver ( $R$ ) (Fig. 1). The following developments will aim at theoretically quantifying the average influence of a given defect position ( $D$ ) on the realizations.

From a practical point of view, it is convenient to analyze the obtained (wide-band) responses using time-frequency analysis or, equivalently, by bandpass filtering in a set of discrete frequency bands.<sup>27</sup> Therefore, the problem can be judiciously treated, without loss of generality, inside an arbitrary frequency band centered on a given frequency  $\omega_0$ . This has the additional virtue of making negligible, as a first approximation, the possible dispersion effects when dealing with guided waves.

Let  $s_{\omega_0}$  be a band-limited, windowed sinusoid signal emitted by the source, of the form  $s_{\omega_0}(t) = w(t) \sin(\omega_0 t)$ , where  $w(t)$  is a windowing function (eg. a Hann window) of duration  $T$ . The response  $h_0(t)$  obtained at the receiver consists of the direct propagation from ( $S$ ) to ( $R$ ) plus an infinite series of reflections on the medium boundaries. This process can be described by a simple shot-noise model. Therefore, as a first approximation,  $h_0$  can thus be considered as a weighted sum of propagated  $s_{\omega_0}$  waveforms. Dividing the time axis into intervals of duration  $\Delta t_i$  centered on regularly spaced instants  $t_i$ , this can be expressed as:

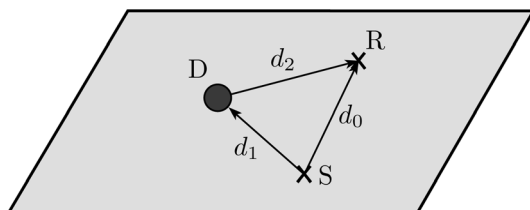


FIG. 1. A given realization of the experiment.

$$h_0(t) = \sum_{i=1}^{\infty} \kappa_i A_i s_{\omega_0}(t - t_i), \quad (1)$$

where  $\kappa_i$  is the number of wavepackets arriving within the  $i$ th time interval and  $A_i = A(t_i)$  is an amplitude term depending on the propagation distance (or, equivalently, the propagation time). This amplitude is associated both to the exponential decrease caused by losses during propagation, with a certain time constant  $\tau$ , and to the two-dimensional geometrical spreading, proportional to the inverse of the square root of the propagation distance. This can be written as  $A(t) = (K/\sqrt{t})e^{-t/\tau}$ , where  $K$  is an arbitrary constant that might indifferently have different values in other frequency bands (other  $\omega_0$  values). It should be noted that the propagation of a single wave type only is considered, which will be acceptable here as it will be seen in Sec. III A.

For a given medium, the distribution of arrival times of the wavepackets contained in  $h_0$  can be determined using the image source method.<sup>34</sup> In order to extract some general trend concerning the reverberant propagation in the medium, a particular set of the source and receiver positions can be considered as a given realization of a random process (similar considerations can be found for instance in.<sup>35</sup> This will be modeled by considering  $\kappa_i$  as an integer random variable. Assuming that the time interval  $\Delta t_i$  is small enough, every  $\kappa_i$  is either 0 or 1, which corresponds to a nonstationary Poisson process of characteristic parameter  $\lambda(t)$ . Physically,  $\lambda$  can be interpreted as the average density of wavepacket arrival times. Hence, it is directly related to the expected value of  $\kappa_i$  in the following way:

$$E[\kappa_i] = \lambda(t_i) \Delta t_i. \quad (2)$$

It is shown in Appendix A that in a two-dimensional case,  $\lambda$  can be approximated by a linear function of time  $\lambda(t) = \beta t$ , where  $\beta$  is a constant depending on the propagation velocity and the medium dimensions.

Now, whenever a defect appears in the medium, the received response is modified and can be written as  $h(t) = h_0(t) + \Delta h(t)$ . Considering the defect as a secondary source,  $\Delta h$  can be expressed in a way similar to Eq. (1):

$$\Delta h(t) = \sum_{j=1}^{\infty} \kappa'_j B_j s_{\omega_0}(t - t_j), \quad (3)$$

with  $\kappa'_j$  the number of arrival times in an interval  $\Delta t_j$  centered at  $t_j$ , and  $B_j = B(t_j) = (K'/\sqrt{t_j})e^{-t_j/\tau}$ .  $K'$  will be supposed equal to  $K' = \alpha K$ , where  $\alpha$  then represents the response of the defect to each incoming wave. The arrival time density associated to  $\Delta h$  is noted  $\lambda'(t)$ . For an arbitrary type of defect,  $\lambda'$  would be *a priori* unknown. We will make here the assumption of a linear dependence with time:  $\lambda'(t) = \gamma t + \varepsilon$ . Details on this point are given in Appendix D (available as supplementary material<sup>37</sup>). It will be verified in Sec. III B that this assumption effectively applies to the experimental situation tested in this study.

As mentioned, the theoretical derivations presented in this paper are based on some simplifying assumptions that have proven to be reasonable. A number of them have

already been discussed above, and some others will be in the next sections. For convenience, they are all listed below:

- 2D geometry;
- single-mode propagation;
- dispersion effects neglected;
- unitary reflection coefficient at the medium boundaries;
- particular defect behavior (linear expression of  $\lambda'$ );
- slow variations of  $A(t)$  and  $\lambda(t)$ ;
- $\kappa_i$  and  $\kappa_j$  independent for  $i \neq j$ ;
- $\kappa_i$  and  $\kappa'_j$  independent for all  $(i, j)$ .

## B. Expected values of the received signal and the envelope

It can be easily shown that the expected value  $E[h_0]$  of the received signal modeled here is zero. Indeed, from Eqs. (1) and (2), the following expression is obtained:

$$E[h_0(t)] = \sum_{i=1}^{\infty} \lambda(t_i) A_i s_{\omega_0}(t - t_i) \Delta t_i. \quad (4)$$

For very small  $\Delta t_i$ , the discrete sum can be converted into an integral ( $\Delta t_i \rightarrow du$ ). Now, remarking that  $s_{\omega_0}(t)$  is zero outside the interval  $[0, T]$  and that  $\lambda(t)$  and  $A(t)$  vary slowly within the duration  $T$  (see eg. Ref. 35 for a similar assumption), a suitable change of variables yields:

$$E[h_0(t)] \simeq \lambda(t) A(t) \int_0^T s_{\omega_0}(u) du = 0. \quad (5)$$

Since the integral of  $s_{\omega_0}$  is zero,  $E[h_0(t)]$  is zero as well. Therefore, no interesting average behavior can be predicted directly from the received response modeled by Eq. (1).

On the contrary, it will be seen that the envelope of  $h_0$  does not vanish by averaging over the realizations. From Eq. (1), the complex analytic representation of  $h_0$  is given by

$$H_0(t) = -j \sum_{i=1}^{\infty} \kappa_i A_i w(t - t_i) e^{j\omega_0(t-t_i)}. \quad (6)$$

Assuming that the random variables  $\kappa_i$  and  $\kappa_j$  are independent for  $i \neq j$ , the expected values of the square of the envelope of  $h_0$  can then be reduced to (see Appendix B for detailed calculation):

$$E[|H_0(t)|^2] \simeq K^2 W^2 \beta e^{-2t/\tau}, \quad (7)$$

where  $W^2 = \int_0^T w^2(t) dt$ .

It will be seen in Sec. III B that this relation can be used to extract basic information on the structure, independently on the relative source and receiver positions.

## C. Influence of a localized defect

In the actually envisaged application, the sources would generate a random acoustic noise. In that case, the received signals would not bring directly exploitable information and only the correlation functions would be insightful. Therefore in this section, it is the correlations that will in fact be con-

sidered as the useful signals. The aim here is then to obtain an estimate of the average influence of the defect's presence on the correlation functions, with respects to the relative locations of the source, the receiver and the defect.

We consider the configuration defined in Fig. 1. Defining  $v$  as the group velocity,  $\tau_0 = d_0/v$  and  $\tau'_0 = (d_1 + d_2)/v$  are respectively the direct source-receiver and source-defect-receiver time-of-flights. In the following,  $\tau_0$  and  $\tau'_0$  will be considered known invariants of the random process, which means that they will be kept constant for every realization. Since the first terms of each sum of Eqs. (1) and (3) correspond to these first arrival times, they will naturally be considered deterministic. Formally, let us define  $i_0$  and  $j_0$  such that  $t_{i_0} = \tau_0$  and  $t_{j_0} = \tau'_0$ . Then by definition,  $\kappa_i = 0$  for  $i < i_0$ ,  $\kappa'_j = 0$  for  $j < j_0$  and  $\kappa_{i_0} = \kappa'_{j_0} = 1$ . For  $i > i_0$  and  $j > j_0$ ,  $\kappa_i$  and  $\kappa'_j$  are 0 or 1, depending on whether a wave-packet arrives at times  $t_i, t_j$  or not.

Following these considerations, the expressions of  $h_0$  and  $\Delta h$  in Eqs. (1) and (3) are separated into deterministic and random parts as

$$h_0(t) = h_0^D(t) + h_0^R(t) \quad (8)$$

and

$$\Delta h(t) = \Delta h^D(t) + \Delta h^R(t), \quad (9)$$

where  $h_0^D(t) = A(\tau_0) s_{\omega_0}(t - \tau_0)$  and  $\Delta h^D(t) = B(\tau'_0) s_{\omega_0}(t - \tau'_0)$  are deterministic, and  $h_0^R(t) = \sum_{i=i_0+1}^{\infty} \kappa_i A_i s_{\omega_0}(t - t_i)$  and  $\Delta h^R(t) = \sum_{j=j_0+1}^{\infty} \kappa'_j B_j s_{\omega_0}(t - t_j)$  are random.

Notating  $\varphi_{h_0 h_0}$  the autocorrelation without defect and  $\varphi_{hh}$  the autocorrelation with a defect, it comes  $\varphi_{hh} = \varphi_{h_0 h_0} + \Delta\varphi$  with  $\Delta\varphi = \varphi_{h_0 \Delta h} + \varphi_{\Delta h h_0} + \varphi_{\Delta h \Delta h}$ .

Considering the autocorrelation function to be the useful signal, the average influence of the defect can then be quantified by the following parameter:

$$r = \frac{E \left[ \int_{-\infty}^{\infty} \Delta\varphi^2(t) dt \right]}{E \left[ \int_{-\infty}^{\infty} \varphi_{h_0 h_0}^2(t) dt \right]}. \quad (10)$$

It represents the ratio between the expected value of the energy of  $\Delta\varphi$ , caused by the presence of the defect, and the expected value of the energy of  $\varphi_{h_0 h_0}$ , the autocorrelation without defect.

Following a mathematical derivation detailed in Appendix C, this parameter can be expressed as

$$r = 2\alpha^2 \frac{P_1(\tau_d)}{Q} e^{-2\tau_d/\tau} + \alpha^4 \frac{P_2(\tau_d)}{Q} e^{-4\tau_d/\tau}, \quad (11)$$

with  $\tau_d = \tau'_0 - \tau_0$  and  $P_1, P_2$ , and  $Q$  defined in Eq. (C9), (C10), and (C11), respectively.

Following the same general derivation, this relation can be easily generalized to the two-receiver case:

$$r_{12} = \alpha^2 \left[ \frac{P'_1}{Q'} e^{-2\tau_{d_2}/\tau} + \frac{P'_2}{Q'} e^{-2\tau_{d_1}/\tau} \right] + \alpha^4 \frac{P'_3}{Q'} e^{-2(\tau_{d_1} + \tau_{d_2})/\tau}, \quad (12)$$

where  $\tau_{d_i} = \tau'_{0_i} - \tau_{0_i}$  ( $i = 1, 2$ ), with  $\tau_{0_i}$  and  $\tau'_{0_i}$ , respectively, the propagation times from the source to the receiver  $i$ , and from the source to the damage to the receiver  $i$ . All details about the derivation and the expressions of  $P'_1$ ,  $P'_2$ ,  $P'_3$ , and  $Q'$  are given in Appendix E (available as supplementary material<sup>37</sup>).

### III. EXPERIMENTAL VALIDATION AND EXPLOITATION

#### A. Experimental setup

The experimental results presented in this section have been obtained on a rectangular aluminum plate of dimensions  $2 \times 1 \text{ m}^2$  and 6 mm thickness. Two piezoelectric transducers (one emitter and one receiver) have been attached at two positions of the plate surface. For practical reasons, and to allow repetitive trials, the defect used here was an aluminum cylinder of 1.25 cm radius coupled on the surface using a viscous gel. The excitation signals  $s_{\omega_0}(t)$  used in this section are 10-cycle, Hanning-windowed sinusoids with frequency in the range [5 – 15 kHz]. The reverberation time for the plate being of the order of 100 ms in this frequency range, experimental signals of 500 ms-duration have been recorded.

Considering the excitation method (surface actuation) and the frequency-plate thickness product, only the flexural (or  $A_0$ ) Lamb mode is expected. Thus the single-mode assumption, implicit in the theoretical derivation, is correct here.

#### B. Parameter estimation

Before using the theoretical expression in Eq. (11) and compare to experimental data, the parameters  $\tau$  and  $\alpha$  have to be determined. They are related respectively to physical properties of the medium and the behavior of the defect, and will be experimentally estimated.

First, the experimental value of  $\tau$  can be estimated using Eq. (7). Precisely, the procedure used here is a curve fitting from a set of functions  $f_{A,\tau}(t) = Ae^{-2t/\tau}$  [as suggested by the form of the function in Eq. (7)]. The retained values of  $A$  and  $\tau$  are those for which  $f_{A,\tau}(t)$  best matches (in the least square sense) the square of the envelope of the measured  $h_0(t)$ . Concretely, we define a cost function  $R(A, \tau) = \sqrt{\sum [y_n - f_{A,\tau}(nT_s)]^2}$  to be minimized, where  $y_n$  are the samples of the squared absolute value of the analytic representation of the measured signal  $h_0$ , computed here using the numerical Hilbert transform implemented in the “signal” package of GNU Octave.<sup>36</sup>  $T_s$  is the sampling period of the acquisition. For measurements performed on the test setup described above,  $R$  reaches its minimum for  $A = 5.7 \cdot 10^{-7}$  and  $\tau = 0.013 \text{ s}$ . Note that the value of  $A$  is of no particular interest in this study. However, both parameters cannot be estimated separately. The result of this curve fitting is presented in Fig. 2. The measured signal  $h_0(t)$  is represented in thin line and the envelope corresponding to the identified  $A$  and  $\tau$  is represented in thick line.

In order to characterize the defect's behavior, a preliminary experiment with a very specific transducers arrange-

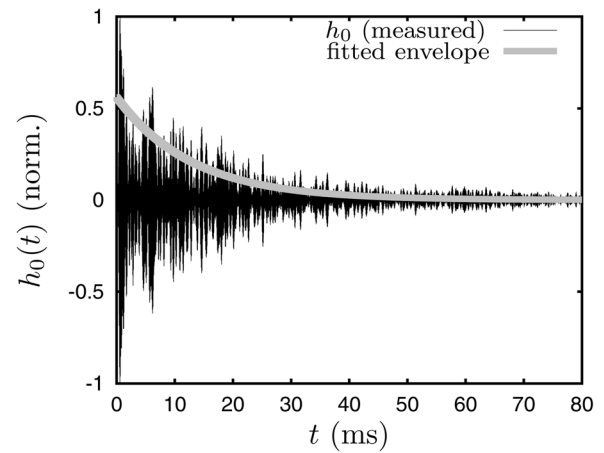


FIG. 2. Curve fitting for parameter identification.

ment has been performed. A source ( $S$ ) and five receivers regularly positioned along a semicircle ( $R_i$ ) have been placed on the plate surface (Fig. 3). The distances between the transducers have been chosen so that the first wavepacket of each received signal is separated from the wavepackets associated to the reflections at the plate edges.

The comparison of the signals  $h_i$  ( $i = 1, \dots, 5$ ) received by the set of receivers when the defect is placed at the center of the semi-circle and the signals  $h_{i_0}$  without the defect then allows to get interesting empirical information about the transmission properties of the defect. Consistently with the definition introduced in Sec. II A, the difference signals are notated  $\Delta h_i = h_i - h_{i_0}$ . First, the ratio of the amplitudes of the first wavepacket of  $\Delta h_1$  and the first wavepacket of  $h_{1_0}$  provides an experimental value of the parameter  $\alpha \simeq 0.59$ .

Then, an estimation of the defect directivity is obtained by plotting the relative amplitudes of the first wavepackets of each  $\Delta h_i$  (Fig. 4). The curve shows that the waves diffracted by the defect are essentially concentrated around the direction of incidence. This effect may be roughly quantified by a divergence angle  $\theta_D \simeq 1.32 \text{ rad}$  estimated using a classical “–3 dB criterion.”

Finally, these experimental considerations enable to build a simple statistical model of the defect's behavior and thus lead to a justification of the linear expression of the arrival time density  $\lambda'(t)$  defined at the end of Sec. II A and used in the theoretical derivation of Sec. II C. All details about this are given in Appendix D (available as supplementary material<sup>37</sup>).

It should be noted that the measurements described here have been repeated several times, the defect being successively removed and placed again, and no significant variations of the results have been observed.

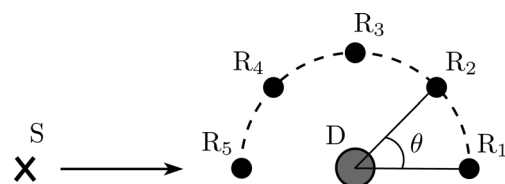


FIG. 3. Measurement of the defect directivity.

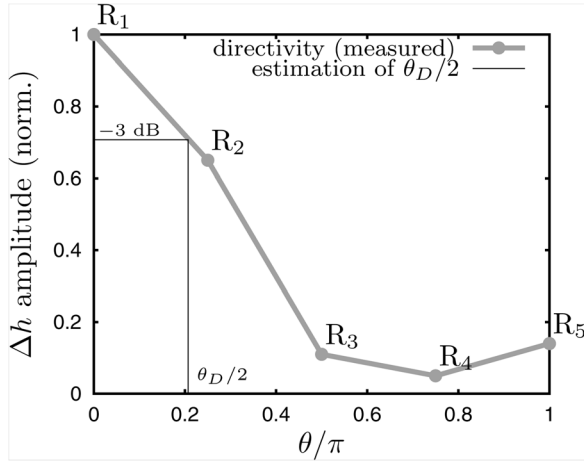


FIG. 4. Measured defect directivity.

**C. Sensitivity to defect position**

The experimental estimations of the parameter  $r$  [defined in Eq. (10)] are computed from the autocorrelations of the received signals, according to the procedure described below. First, the experimental received signal  $h_0(t)$  in the damage-free plate is measured for fixed source and receiver positions. Then, the received signals  $h(t)$  are measured for different defect positions, randomly chosen in such a way as to cover the plate surface, and all the autocorrelations and energy ratios are computed. Finally, the expected values are estimated by averaging these ratios per interval of  $\tau_d$ .

The obtained results are presented in Fig. 5, and compared to the theoretical expression given in Eq. (11). A very satisfying agreement is obtained. This shows that the theoretical developments of Sec. II C allow a correct prediction of the evolution of the defect’s influence on the correlation as a function of the defect’s position.

The major interest of these results is in the design of the passive monitoring system envisaged. Considering some threshold value  $r_t$  for the sensitivity, the damage would be considered “detectable” by a given sensor if  $r > r_t$ . On the contrary,  $r < r_t$  would mean that the measured correlation function would be virtually unaffected by the defect’s pres-

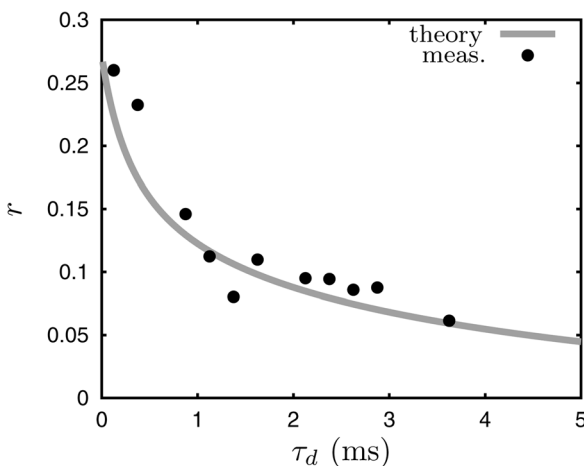


FIG. 5. Evolution of  $r$  as a function of  $\tau_d$ : theoretical expression (solid line) of Eq. (11) and experimental values (dots).

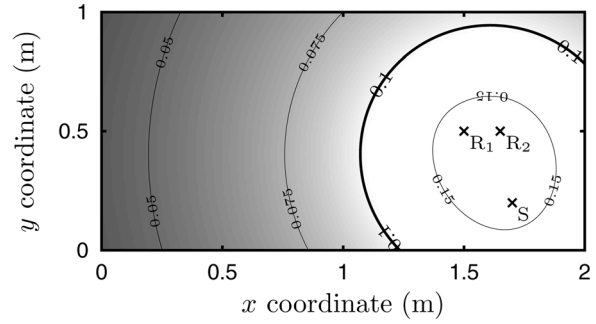


FIG. 6. Definition of the monitoring area.

ence, and then would make the corresponding sensor a good candidate for the source configuration identification (reference sensor).

To illustrate this on a practical case, we consider two sensors  $R_1$  and  $R_2$  and a source  $S$  located at given (fixed) positions of the plate. The sensitivity of the cross-correlation to a defect of coordinates  $(x, y)$  can be theoretically estimated using Eq. (12). Then, by representing the value of  $r_{12}$  in gray level for each  $(x, y)$  on the discretized plate surface (2D-grid), a map of the sensitivity to the defect can be established for the particular measurement configuration (Fig. 6).

Empirically, the modification of the measured correlation has proven clearly observable for  $r > 0.1$ .<sup>27,29,30</sup> Then the level curve for the threshold value  $r_t = 0.1$  has been displayed in thicker line. The white area inside this curve can thus be interpreted as the “monitoring area” for sensors  $R_1$  and  $R_2$ , where the occurrence of a given damage would be detected. On the contrary, a damage appearing in the grayed area outside this curve would be virtually undetectable.

In a similar way, a map of acceptable reference sensor locations can be obtained using Eq. (11). We consider here a defect ( $D$ ) located approximately at the center of the monitoring area defined above. Now the variable coordinates  $(x, y)$  are those of a “candidate” reference sensor. The sensitivity of the autocorrelation to the damage (the value of  $r$ ) as a function of  $(x, y)$  is represented on Fig. 7. Here again, the level curve for  $r = r_t$  is emphasized. The only acceptable locations for the sensor are in the grayed area outside this curve.

This provides a theoretical justification of the results already observed in Ref. 27, where the reference sensor and the damage appear to have been located inside the areas defined above. This naturally explains both the unequivocal

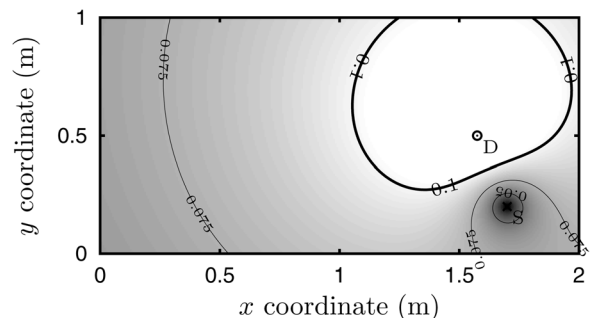


FIG. 7. Positioning of the reference sensor.

detectability of the damage by the two measurement sensors and the relative insensitivity of the third (reference) sensor.

#### IV. CONCLUSION AND FUTURE WORK

The results presented and discussed in this paper constitute an important step toward a passive SHM system based on ambient acoustic field correlation. The particularity here is that the application of the principle has been demonstrated even in nondiffuse and nonstationary field conditions.

The statistical model developed has shown how the average influence of a localized defect on the correlation functions is guided by a limited number of parameters: the reverberation properties of the medium, the radiation characteristics of the damage and the relative positions of the source, the receiver and the defect. The theoretical predictions, obtained in a single-mode and two-dimensional propagation situation, have been successfully confronted to measurements and their use has been illustrated on a typical case study.

However, a lot of theoretical work has still to be done before developing a fully functional passive SHM system. In particular, taking into account actual scattering properties of defects and multimode propagation would lead to a more complete model, adapted to more general practical situations. In the same idea, dealing not only with reverberant, but also media with scattering and even multiscattering properties could be pertinent. Such extensions of the modeling could be very precious, in order to go beyond the mere damage detection and envisage localization, characterization or even, ultimately, imaging in a fully passive way.

#### ACKNOWLEDGMENTS

The authors would like to thank Dr. Eric Larose from ISTerre and Dr. Julien de Rosny from Institut Langevin for stimulating discussions and helpful suggestions on this work.

#### APPENDIX A: ESTIMATION OF $\lambda(t)$ FOR A RECTANGULAR PLATE

Let us consider a rectangular plate of surface  $\mathcal{S}$  (represented by the solid lines in Fig. 8). The images of the primary source (emitter position) are located according to a periodic pattern, whose elementary cell is the dashed-line rectangle represented in Fig. 8.<sup>34</sup>

Each image source will generate its own wavepacket eventually arriving at the receiver. The ones located inside a disk of radius  $\rho$  will then produce wavepackets arriving before the time  $t = \rho/v$ , where  $v$  is the group velocity of the propagation in the medium. The number  $\Lambda(\rho)$  of these image sources is four times the number of elementary cells included in the disk. For  $\rho$  much greater than the plate dimensions, it corresponds approximately to the ratio of the disk surface and the plate surface:

$$\Lambda(\rho) \simeq \frac{\pi\rho^2}{\mathcal{S}} \quad (\text{A1})$$

Obviously, this can also be interpreted as the number of wavepackets arriving before time  $t$ :

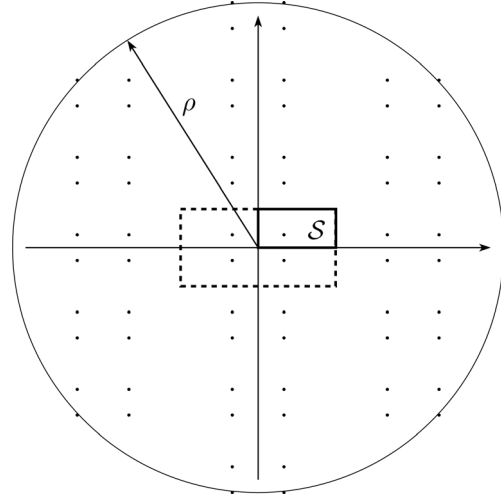


FIG. 8. Image sources for a rectangular plate.

$$\Lambda(t) \simeq \frac{\pi v^2 t^2}{\mathcal{S}} \quad (\text{A2})$$

Then, the number of wavepackets arriving between  $t$  and  $t + dt$  is  $\Lambda(t + dt) - \Lambda(t) = d\Lambda$ . The arrival time density  $\lambda$  is defined as:

$$\lambda(t) = \frac{d\Lambda}{dt} \quad (\text{A3})$$

From Eq. (A2),  $\lambda$  can then be estimated as:

$$\lambda(t) \simeq \beta t \quad (\text{A4})$$

with

$$\beta = \frac{2\pi v^2}{\mathcal{S}} \quad (\text{A5})$$

#### APPENDIX B: THEORETICAL DERIVATION OF THE ENVELOPE OF $h_0$

From Eq. (6), the square of the envelope of  $h_0(t)$  is

$$\begin{aligned} |H_0(t)|^2 &= \left[ \sum_{i=1}^{\infty} \kappa_i A_i w(t - t_i) \cos[\omega_0(t - t_i)] \right]^2 \\ &\quad + \left[ \sum_{i=1}^{\infty} \kappa_i A_i w(t - t_i) \sin[\omega_0(t - t_i)] \right]^2 \\ &= \sum_{i=1}^{\infty} \sum_{j=1}^{\infty} \kappa_i \kappa_j A_i A_j w(t - t_i) w(t - t_j) \cos[\omega_0(t_j - t_i)] \end{aligned} \quad (\text{B1})$$

Separating in the double sum above the terms with  $i = j$  and the cross-terms, and taking the expected value then yields:

$$\begin{aligned} E[|H_0(t)|^2] &= \sum_i E[\kappa_i^2] A_i^2 w^2(t - t_i) \\ &\quad + \sum_i \sum_{j \neq i} E[\kappa_i \kappa_j] A_i A_j w(t - t_i) w(t - t_j) \\ &\quad \times \cos[\omega_0(t_j - t_i)]. \end{aligned} \quad (\text{B2})$$

Assuming that the random variables  $\kappa_i$  and  $\kappa_j$  are independent for  $i \neq j$  and remarking that  $\kappa_i^2 = \kappa_i$  (since it is either 0 or 1) the expected values in the equation above can be simplified to

$$E[\kappa_i \kappa_j] = E[\kappa_i]E[\kappa_j] = \lambda(t_i)\lambda(t_j)\Delta t_i \Delta t_j \quad (\text{B3})$$

for  $i \neq j$ , and

$$E[\kappa_i^2] = E[\kappa_i] = \lambda(t_i)\Delta t_i. \quad (\text{B4})$$

Replacing the discrete sums in Eq. (B2) by integrals ( $\Delta t_i \rightarrow du$ ,  $\Delta t_j \rightarrow dv$ ) then yields:

$$\begin{aligned} E[|H_0(t)|^2] &= \int_0^{+\infty} \lambda(u)A^2(u)w^2(t-u)du \\ &+ \int_0^{+\infty} \int_0^{+\infty} \lambda(u)\lambda(v)A(u)A(v)w(t-u) \\ &\times w(t-v) \cos[\omega_0(v-u)]dudv. \end{aligned} \quad (\text{B5})$$

Using once more the fact that  $w(t)$  is zero outside the interval  $[0, T]$  and that  $\lambda(t)$  and  $A(t)$  vary slowly, and after performing the suitable change of variables, Eq. (B5) becomes

$$\begin{aligned} E[|H_0(t)|^2] &\simeq \lambda(t)A^2(t) \int_0^T w^2(u)du \\ &+ \lambda^2(t)A^2(t) \int_0^T \int_0^T w(u)w(v) \\ &\times \cos[\omega_0(v-u)]dudv. \end{aligned} \quad (\text{B6})$$

Splitting the cosine and then separating the variables in the double integral term above yields

$$\begin{aligned} &\int_0^T \int_0^T w(u)w(v) \cos[\omega_0(v-u)]dudv \\ &= \left[ \int_0^T w(t) \cos(\omega_0 t) dt \right]^2 + \left[ \int_0^T w(t) \sin(\omega_0 t) dt \right]^2. \end{aligned} \quad (\text{B7})$$

Typically, the window function  $w(t)$  could be for instance a Hann window function expressed as

$$w(t) = \begin{cases} \frac{1 - \cos(\omega_0 t/N_c)}{2} & \text{if } 0 \leq t \leq T, \\ 0 & \text{if } t > T \end{cases}, \quad (\text{B8})$$

where  $N_c$  is the number of sinusoid cycles.

Then, reporting the expression in Eq. (B8) into Eq. (B7), it is easy to show that both terms are zero. Note that the same conclusion can naturally be reached with other classical window types (rectangular, Hamming, Blackman,...) as well. This shows that the cross-term influence may be ignored, as already observed elsewhere.<sup>7</sup>

Therefore, Eq. (B6) simply reduces to

$$E[|H_0(t)|^2] \simeq \lambda(t)A^2(t)W^2 = K^2W^2\beta e^{-2t/\tau} \quad (\text{B9})$$

where  $W^2 = \int_0^T w^2(t)dt$  is the energy of the windowing function (the envelope)  $w(t)$  of the emitted signal  $s_{\omega_0}(t)$ .

## APPENDIX C: DERIVATION OF THE DEFECT SENSITIVITY PARAMETER $r$

From Eqs. (8) and (9), the first term of  $\Delta\varphi$  can be expressed as

$$\begin{aligned} \varphi_{h_0\Delta h}(t) &= A(\tau_0)B(\tau'_0)\varphi_{\omega_0}(t - \tau'_0 + \tau_0) \\ &+ A(\tau_0) \sum_{j=j_0+1}^{\infty} \kappa'_j B_j \varphi_{\omega_0}(t + \tau_0 - t_j) \\ &+ B(\tau'_0) \sum_{i=i_0+1}^{\infty} \kappa_i A_i \varphi_{\omega_0}(t + t_i - \tau'_0) \\ &+ \sum_{i=i_0+1}^{\infty} \sum_{j=j_0+1}^{\infty} \kappa_i \kappa'_j A_i B_j \varphi_{\omega_0}(t + t_i - t_j) \end{aligned} \quad (\text{C1})$$

where  $\varphi_{\omega_0}$  is the autocorrelation of  $s_{\omega_0}$ .

In the same way that in Eq. (B6), the cross-terms once more give vanishing contributions when taking the square of Eq. (C1). Then, since  $\kappa_i^2 = \kappa_i$  and  $\kappa'_j{}^2 = \kappa'_j$ , the energy of the correlation function can be written as

$$\begin{aligned} \int_{-\infty}^{+\infty} \varphi_{h_0\Delta h}^2(t)dt &= A^2(\tau_0)B^2(\tau'_0) \int_{-\infty}^{+\infty} \varphi_{\omega_0}^2(t - \tau'_0 + \tau_0)dt \\ &+ A^2(\tau_0) \sum_j \kappa'_j B_j^2 \int_{-\infty}^{+\infty} \varphi_{\omega_0}^2(t + \tau_0 - t_j)dt \\ &+ B^2(\tau'_0) \sum_i \kappa_i A_i^2 \int_{-\infty}^{+\infty} \varphi_{\omega_0}^2(t + t_i - \tau'_0)dt \\ &+ \sum_i \sum_j \kappa_i \kappa'_j A_i^2 B_j^2 \int_{-\infty}^{+\infty} \varphi_{\omega_0}^2(t + t_i - t_j)dt \end{aligned} \quad (\text{C2})$$

By performing suitable changes of variables, it is easy to show that all integral terms in Eq. (C2) merely reduce to the energy of the autocorrelation of  $s_{\omega_0}$ , defined as  $\Phi_{\omega_0}^2 = \int_{-T}^T \varphi_{\omega_0}^2(t)dt$ . Then, in a similar way as in the previous section, taking the expected value, assuming that  $\kappa_i$  and  $\kappa'_j$  are independent, and replacing the discrete sums by integrals yield:

$$\begin{aligned} &E \left[ \int_{-\infty}^{+\infty} \varphi_{h_0\Delta h}^2(t)dt \right] \\ &= \Phi_{\omega_0}^2 \left[ A^2(\tau_0)B^2(\tau'_0) + A^2(\tau_0) \int_{\tau'_0}^{+\infty} \lambda'(v)B^2(v)dv \right. \\ &\quad + B^2(\tau'_0) \int_{\tau_0}^{+\infty} \lambda(u)A^2(u)du \\ &\quad \left. + \int_{\tau_0}^{+\infty} \int_{\tau'_0}^{+\infty} \lambda(u)\lambda'(v)A^2(u)B^2(v)dudv \right]. \end{aligned} \quad (\text{C3})$$

Introducing the expressions of  $\lambda$  and  $\lambda'$  established in Appendices A and D (available as supplementary material<sup>37</sup>), Eqs. (A4) and (D6) in Eq. (C3) yields:

$$E \left[ \int_{-\infty}^{+\infty} \varphi_{h_0 \Delta h}^2(t) dt \right] = \Phi_{\omega_0}^2 \alpha^2 K^4 e^{-2(\tau_0 + \tau'_0)/\tau} \left[ \frac{1}{\tau_0 \tau'_0} + \frac{\gamma \tau}{2\tau_0} + \frac{\beta \tau}{2\tau'_0} \right. \\ \left. + \frac{\gamma \beta \tau^2}{4} - \varepsilon e^{2\tau'_0/\tau} \left( \frac{1}{\tau_0} + \frac{\beta \tau}{2} \right) \text{Ei}(-2\tau'_0/\tau) \right], \quad (\text{C4})$$

where  $\text{Ei}(x) = \int_{-\infty}^x (e^t/t) dt$  is the exponential integral function.

Once more neglecting the cross-terms, the energy ratio  $r$  defined in Eq. (10) is then given by

$$r = \frac{2E \left[ \int_{-\infty}^{\infty} \varphi_{h_0 \Delta h}^2(t) dt \right] + E \left[ \int_{-\infty}^{\infty} \varphi_{\Delta h \Delta h}^2(t) dt \right]}{E \left[ \int_{-\infty}^{\infty} \varphi_{h_0 h_0}^2(t) dt \right]} \quad (\text{C5})$$

Performing the same kind of calculation as from Eqs. (C1) to (C4), the other terms  $E \left[ \int_{-\infty}^{+\infty} \varphi_{\Delta h \Delta h}^2(t) dt \right]$  and  $E \left[ \int_{-\infty}^{+\infty} \varphi_{h_0 h_0}^2(t) dt \right]$  of Eq. (C5) can be expressed as

$$E \left[ \int_{-\infty}^{+\infty} \varphi_{\Delta h \Delta h}^2(t) dt \right] = \Phi_{\omega_0}^2 \alpha^4 K^4 e^{-4\tau'_0/\tau} \left[ \frac{1}{\tau_0'^2} + \frac{\gamma \tau}{\tau'_0} + \frac{\gamma^2 \tau^2}{4} \right. \\ \left. - \varepsilon e^{2\tau'_0/\tau} \left( \frac{2}{\tau'_0} + \gamma \tau \right) \text{Ei}(-2\tau'_0/\tau) \right. \\ \left. + \varepsilon^2 e^{4\tau'_0/\tau} \text{Ei}^2(-2\tau'_0/\tau) \right] \quad (\text{C6})$$

and

$$E \left[ \int_{-\infty}^{+\infty} \varphi_{h_0 h_0}^2(t) dt \right] = \Phi_{\omega_0}^2 K^4 e^{-4\tau_0/\tau} \left[ \frac{1}{\tau_0^2} + \frac{\beta \tau}{\tau_0} + \frac{\beta^2 \tau^2}{4} \right] \quad (\text{C7})$$

Introducing Eqs. (C4), (C6), and (C7) into Eq. (C5) then yields:

$$r = 2\alpha^2 \frac{P_1(\tau_d)}{Q} e^{-2\tau_d/\tau} + \alpha^4 \frac{P_2(\tau_d)}{Q} e^{-4\tau_d/\tau} \quad (\text{C8})$$

with

$$P_1(\tau_d) = \frac{1}{\tau_0(\tau_0 + \tau_d)} + \frac{\gamma \tau}{2\tau_0} + \frac{\beta \tau}{2(\tau_0 + \tau_d)} + \frac{\gamma \beta \tau^2}{4} \\ - \varepsilon e^{2(\tau_0 + \tau_d)/\tau} \left( \frac{1}{\tau_0} + \frac{\beta \tau}{2} \right) \text{Ei} \left( -2 \frac{\tau_0 + \tau_d}{\tau} \right) \quad (\text{C9})$$

$$P_2(\tau_d) = \frac{1}{(\tau_0 + \tau_d)^2} + \frac{\gamma \tau}{\tau_0 + \tau_d} + \frac{\gamma^2 \tau^2}{4} \\ - \varepsilon e^{2(\tau_0 + \tau_d)/\tau} \left( \frac{2}{\tau_0 + \tau_d} + \gamma \tau \right) \text{Ei} \left( -2 \frac{\tau_0 + \tau_d}{\tau} \right) \\ + \varepsilon^2 e^{4(\tau_0 + \tau_d)/\tau} \text{Ei}^2 \left( -2 \frac{\tau_0 + \tau_d}{\tau} \right) \quad (\text{C10})$$

and

$$Q = \frac{1}{\tau_0'^2} + \frac{\beta \tau}{\tau_0} + \frac{\beta^2 \tau^2}{4}, \quad (\text{C11})$$

where  $\tau_d = \tau'_0 - \tau_0$ .

- <sup>1</sup>Y. Lu and J. E. Michaels, *IEEE Trans. Ultrason. Ferroelectr. Freq. Control* **55**, 173 (2008).
- <sup>2</sup>A. Aubry and A. Derode, *J. Appl. Phys.* **106**, 044903 (2009).
- <sup>3</sup>E. Larose, T. Planes, V. Rossetto, and L. Margerin, *Appl. Phys. Lett.* **96**, 204101 (2010).
- <sup>4</sup>E. Larose, A. Derode, M. Campillo, and M. Fink, *J. Appl. Phys.* **95**, 8393 (2004).
- <sup>5</sup>A. Derode, A. Tourin, and M. Fink, *J. Appl. Phys.* **85**, 6343 (1999).
- <sup>6</sup>M. Cowan, I. Jones, J. Page, and D. Weitz, *Phys. Rev. E* **65**, 066605 (2002).
- <sup>7</sup>R. Snieder, *Pure Appl. Geophys.* **163**, 455 (2006).
- <sup>8</sup>J. E. Michaels, Y. Lu, and T. E. Michaels, *Proc. SPIE* **5768** 97 (2005).
- <sup>9</sup>A. Grêt, R. Snieder, and U. Özbay, *Geophys. J. Int.* **167**, 504 (2006).
- <sup>10</sup>M. M. Haney, K. van Wijk, L. A. Preston, and D. F. Aldridge, *Leading Edge* **28**, 554 (2009).
- <sup>11</sup>J. de Rosny, P. Roux, M. Fink, and J. H. Page, *Phys. Rev. Lett.* **90**, 094302 (2003).
- <sup>12</sup>V. Bertaix, J. Garson, N. Quieffin, S. Catheline, J. de Rosny, and M. Fink, *Am. J. Phys.* **72**, 1308 (2004).
- <sup>13</sup>P. Roux, W. A. Kuperman, and T. N. Group, *J. Acoust. Soc. Am.* **116**, 1995 (2004).
- <sup>14</sup>K. G. Sabra, P. Roux, and W. A. Kuperman, *J. Acoust. Soc. Am.* **117**, 164 (2005).
- <sup>15</sup>K. G. Sabra, P. Roux, and W. A. Kuperman, *J. Acoust. Soc. Am.* **118**, 3524 (2005).
- <sup>16</sup>S. E. Fried, W. A. Kuperman, K. G. Sabra, and P. Roux, *J. Acoust. Soc. Am.* **124**, EL183 (2008).
- <sup>17</sup>N. M. Shapiro and M. Campillo, *Geophys. Res. Lett.* **31**, L07614, doi:10.1029/2004GL019491 (2004).
- <sup>18</sup>N. M. Shapiro, M. Campillo, L. Stehly, and M. Ritzwoller, *Science* **29**, 1615 (2005).
- <sup>19</sup>K. G. Sabra, P. Gerstoft, P. Roux, W. Kuperman, and M. C. Fehler, *Geophys. Res. Lett.* **32**, L023155 (2005).
- <sup>20</sup>R. L. Weaver, *J. Acoust. Soc. Am.* **71**, 1608 (1982).
- <sup>21</sup>O. Lobkis and R. Weaver, *J. Acoust. Soc. Am.* **110**, 3011 (2001).
- <sup>22</sup>R. Weaver and O. Lobkis, *J. Acoust. Soc. Am.* **116**, 2731 (2004).
- <sup>23</sup>K. Wapenaar, *Phys. Rev. Lett.* **93**, 254301 (2004).
- <sup>24</sup>K. Sabra, E. Winkel, D. Bourgoyne, B. Elbing, S. Ceccio, M. Perlin, and D. Dowling, *J. Acoust. Soc. Am.* **121**, 1987 (2007).
- <sup>25</sup>E. Larose, P. Roux, and M. Campillo, *J. Acoust. Soc. Am.* **122**, 3437 (2007).
- <sup>26</sup>K. Sabra, A. Srivastava, F. L. di Scalea, I. Bartoli, P. Rizzo, and S. Conti, *J. Acoust. Soc. Am.* **123**, EL8 (2008).
- <sup>27</sup>E. Moulin, N. Abou Leyla, J. Assaad, and S. Grondel, *Appl. Phys. Lett.* **95**, 094104 (2009).
- <sup>28</sup>C. Hadziioannou, E. Larose, O. Coutant, P. Roux, and M. Campillo, *J. Acoust. Soc. Am.* **125**, 3688 (2009).
- <sup>29</sup>N. Abou Leyla, E. Moulin, J. Assaad, S. Grondel, and P. Poussot, in *Program abstracts Acoustics'08*, *J. Acoust. Soc. Am.*, Vol. 123 (Paris, France, 2008), p. 3698.
- <sup>30</sup>N. Abou Leyla, E. Moulin, J. Assaad, S. Grondel, and C. Delebarre, in *Program abstracts 157th ASA Meeting*, *J. Acoust. Soc. Am.*, Vol. 125 (Portland, OR, 2009), p. 2635.
- <sup>31</sup>C. Draeger and M. Fink, *J. Acoust. Soc. Am.* **105**, 611 (1999).
- <sup>32</sup>R. K. Ing, N. Quieffin, S. Catheline, and M. Fink, *Appl. Phys. Lett.* **87**, 204104 (2005).
- <sup>33</sup>G. Ribay, S. Catheline, D. Clorennec, R. K. Ing, N. Quieffin, and M. Fink, *IEEE Trans. Ultrason. Ferroelectr. Freq. Control* **54**, 378 (2007).
- <sup>34</sup>J. Cuenca, F. Gautier, and L. Simon, *J. Sound Vib.* **322**, 1048 (2009).
- <sup>35</sup>C. Draeger, J.-C. Aime, and M. Fink, *J. Acoust. Soc. Am.* **105**, 618 (1999).
- <sup>36</sup>GNU Octave <http://www.octave.org> (date last viewed 07/2021/10) and extra packages <http://octave.sourceforge.net/packages.php> (date last viewed 07/21/10).
- <sup>37</sup>See supplementary material at <http://dx.doi.org/10.1063/1.3652907> for Appendixes D and E.